International Journal of Automotive Technology, Vol. 6, No. 5, pp. 467–473 (2005)

1229–9138/2005/023–05

CONCEPTUAL DESIGN OF INNER-SPHERICAL CONTINUOUSLY VARIABLE TRANSMISSION FOR BICYCLE USAGE

S. H. SEONG*, J. H. RYU, H. W. LEE and N. G. PARK

Department of Mechanical Design Engineering, Pusan National University, Busan 609-735, Korea

(Received 4 March 2004; Revised 21 June 2004)

ABSTRACT–A continuously variable transmission (CVT) with an inner spherical traction drive was conceptually designed for bicycle usage. The range of the overall speed ratio is from 1.0 to 4.5. The rated power and pedal speed are 100 Watts and 6 rad/s, respectively. The peculiar packageability, high-level power efficiency and high torque capacity were considered in the design process. A compact CVT that can be installed within a $244 \times 125 \times 160$ mm^3 space and is above 0.9 in efficiency for the rated values was numerically designed. The distribution of efficiency according to the input torque and input speed were calculated. Gradeability in the prescribed operation mode was simulated.

KEY WORDS : Inner-spherical CVT, Infinitely variable transmission, Continuously variable unit, Transmission performance, Power efficiency, OSR, Acceleration, Gradeability

1. INTRODUCTION

Since the CVT is more drivable and controllable than gear transmissions, research and development for the vehicle usage of CVT has been gradually increasing. The typical bicycle transmission is the chain sprocket type. When the chain is shifted to the neighboring sprocket in motion, it frequently derails. A few researchers have developed CVTs for bicycles, but these have not significantly improved bicycle operation because the installation's narrowness and compactness requires high power efficiency for the rider's comfort, as well as large torque capacity due to the slow pedal speed (about 6 rad/s at the rated power of 100 W). For the same reason, there are few published papers referencing CVT development. Recently, J. Kim, *et al.* proposed a spherical type of CVT connecting a sphere with four discs (J. Kim, 2002; J. Kim, 2003). A conceptual model having a very small torque capacity (about 0.1 Nm) was investigated numerically and experimentally. However, this model might be difficult to apply to the bicycle.

The scarcity of published reports for CVTs for bicycles is in contrast to the many investigations conducted into automobile CVTs with belts or traction drives (Tanaka, 1991; Tanaka, 1996; Shoji, 2003; Carter, 2003). These studies have mainly focused on improving power density for fuel economy (Pfiffner, 2003; Lee, 2003). However, in the bicycle CVT (BCVT) design, the most significant design concept is maintaining the comfort of the rider through narrow-compact packageability and high power efficiency.

To develop a BCVT satisfying the required design specifications listed in this paper, a new inner-spherical type of CVT (ISCVT) is proposed. The input and output rotors are kinematically connected with a four-bar linkage as a relay to the counter rotor assembly, which is the position device. Each pair of rotors consists of two partially prepared spherical rotors of which the inner and outer surfaces contact at a single point.

The proposed mechanism has three advantages compared to the toroidal mechanism. The first advantage in terms of power transmissibility. In the proposed mechanism, the concave-convex contacting is superior to the convex-convex one in the toroidal mechanism because the former has a larger contact area than the latter under the same maximum contact pressures. The second advantage is due to the shape of the contact area. The shape of the contact area of the ISCVT is always circular, compared to the elliptical toroidal CVT. When the contact area is circular, the power loss due to the spin rotation is less than for elliptical contact. The last advantage is the four-bar linkage in the proposed model removes the counter rotor assembly at the desired position, which means that there are two centers of the four spherical traction drives, the drive, driven and two conjugated counter rotor surfaces. This mechanism was introduced in the papers of N. G. Park (Ryu, 2002). With this mechanism, it is possible to design an infinitely

*Corresponding author. e-mail: slshoon@hanmail.net

variable transmission (IVT). The overall speed ratio of the CVT can be expanded infinitely according to the crank and follower locations, respectively.

These three advantages (high power transmissibility, low spin loss, and large coverage of overall speed ratio) make it possible to obtain several feasible solutions for satisfying the aforementioned peculiar design specifications for bicycle usage. The object of this study was to design the ISCVT for a bicycle. A kinematical analysis was completed to evaluate the design specifications such as the overall speed ratio (OSR) and interferences among the components of the mechanism. The kinetic analysis also calculated the overall power efficiency under the condition of dry contact of two steel bodies. Several aspects of transmission performance were examined numerically during the simulations.

2. PROPOSED MECHANISM FOR CVT

A pairing of spherical CVTs at the inner and outer surfaces is proposed for bicycle use. A schematic diagram is shown in Figure 1.

The bicycle ISCVT consists of four parts, two belt drives, two sets of traction rotors, two pressure devices, and a ratio changer. The front-belt drive transfers the input power from the pedal to the input shaft of the continuously variable unit (CVU). The rear-belt drive transfers the output power from the CVU to the rear wheel. Timing belts with over-95% efficiency are used.

The input power transfers to the spherical-type driving rotor containing a frontal pressure device. The drive rotor axially slides to the drive shaft connected to the input pulley. Between the drive rotor and the drive shaft end, a rubber spring is inserted, which is the frontal pressure device to generate the constant contact force at the driving traction rotor pair. The thrust force is preloaded and calibrated with a bolt-nut device and a rubber spring.

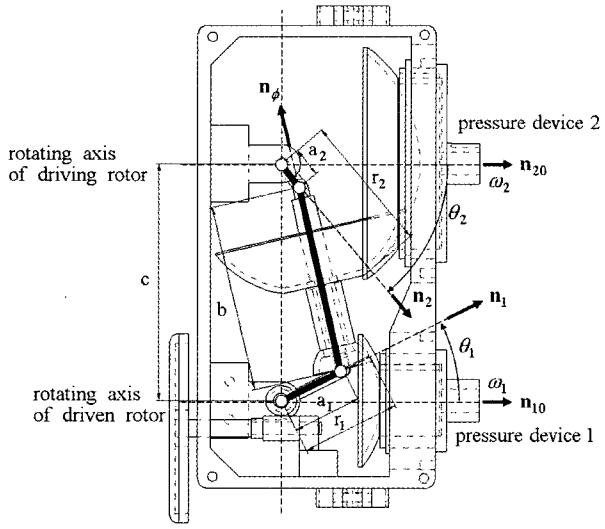

Figure 1. Schematic diagram of the CVT.

The traction area is located on the inner face of the spherical rotor. The counter rotor is also spherical, but with an outer traction surface. The two spheres are installed so that the centers are on the line of the normal of the contact area. The center of the inner spherical rotor (drive rotor) is on the same rotating axis and fixed. That is, one of the outer spherical rotors (the counter rotor) is between one of the inner spherical rotors and the contact point of two rotors but moves with the line of the contact normal. The contact normal direction is varied by the crank link of the four-bar linkage, which is a component of the ratio changer. Since the pivot of the crank is located at the center of the outer spherical rotor and the joint with the coupler is also located at the center of the outer spherical rotor, there is no dead zone resulting from self-rocking between the two rotors.

The other outer spherical rotor and the associated driven rotor are paired with the same mechanism. The center of the inner sphere of the driven rotor is located on its rotating axis. The center of the other outer spherical rotor, as is the other counter rotor, is on the joint between the coupler link and the follower link. Two counter rotors of the drive and driven parts are directly connected and rotated on the coupler link. There is a pressure device between the driven rotor and the driven pulley of the same type as that of the frontal pressure device. The two pressure devices generate constant axial loads, as well as associated normal forces to the contact areas. The angle of crank is controlled by the handle grips device connected with steel wires and a back spring installed within the case of the CVU.

The 4-bar linkage controls the location of the counter rotor assembly by continuously changing the speed, using the control lever to transform the crank angle. Pressure is applied by the tightening of the bolts. The kinematic relationships among the crank, follower, and coupler angles are as follows:

$$a_1 \cos\theta_1 + b \cos\phi = c \sin\alpha + a_2 \cos\theta_2 \tag{1}$$

$$a_1 \sin\theta_1 + b \sin\phi = c \cos\alpha + a_2 \sin\theta_2 \tag{2}$$

where a_1, a_2, b and c are the lengths of the crank, the follower, the coupler and the fixed link, θ_1 and θ_2 are the angles of the crank and the follower, and α and ϕ are the angles of the fixed link and the coupler.

Since the 4-bar linkage is a mechanism with one degree of freedom, the speed ratio of the CVU is defined as the output speed ratio with respect to the input speed as a function of the crank angle. The speed ratio is expressed as follows:

$$\delta = \frac{r_1 \sin\theta_1}{(r_1 - a_1)\sin(\phi - \theta_1)} \frac{r_2 \sin\theta_2}{(r_2 - a_2)\sin(\phi - \theta_2)} \tag{3}$$

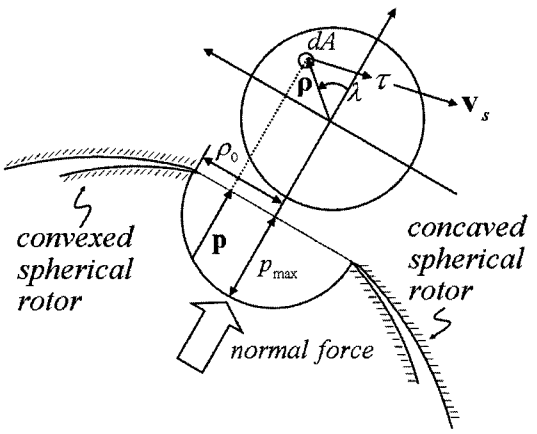

Figure 2. Hertzian contact model.

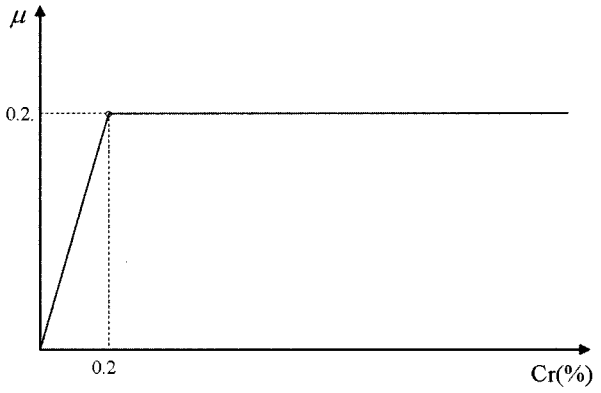

Figure 3. Simple friction model.

where $\delta \equiv \omega_2/\omega_1$ is the OSR and r_1 and r_2 are the radii of the drive and the driven traction rotor, respectively.

A simple contact model based on the Hertzian theory (Norton, 2000), as shown in Figure 2, was considered for the analysis of transmission performances. Normal pressure in an infinitesimal area is defined as follows:

$$\mathbf{p} = p\mathbf{n}_1 \tag{4}$$

$$p = p_{\max}\sqrt{1-\left(\frac{|\rho|}{\rho_0}\right)^2} \tag{5}$$

where $\mathbf{p}$ is the normal pressure vector in the infinitesimal area, and ρ is the local position vector of the infinitesimal area dA_1.

There is some spin and creep in the contact area, and the direction of the shear stress is assumed to coincide with the direction of the sliding velocity between the two bodies:

$$\tau = \mu p\frac{\mathbf{v}_s}{|\mathbf{v}_s|} \tag{6}$$

where τ is the shear pressure vector in the infinitesimal area, μ is the traction coefficient, and $\mathbf{v}_s$ is the sliding velocity.

Simplifying the friction model (as shown in Figure 3), which has a friction coefficient of about 0.2 on the steel-steel dry contact, we have

$$\mu = \mu(c_r) \tag{7}$$

$$c_r = \frac{|\mathbf{v}_s|}{|\mathbf{v}_1|} \tag{8}$$

where c_r is the creep rate, and $\mathbf{v}_1$ is the velocity of the contact point at the drive part.

Since the friction coefficient is a function of the creep rate, which is defined as the ratio of the sliding speed versus the rolling speed of the rotor, the mechanism of the contact phenomena is implicitly related to the coupling between the rotating speeds and transmitted torques of the rotors. Thus, two nonlinear algebraic equations based on the moment equilibrium conditions of the rotors are formulated and solved to estimate the overall energy efficiency and the associated transmission performances. The algorithm used to analyze the transmission performances is as follows.

Step 1. The radii of inner spherical rotors and of the associated outer spherical rotors, the dimensions of the four-bar linkage, the friction coefficients, and the material properties of the contact bodies are prescribed. The limits of the environmental parameters (pedal torque as the input torque, pedal speed as the input speed, and the OSR) are also prescribed in order to calculate the transmission performance (the energy efficiency, the maximum contact shear stresses, and the torque driving the crank angle). The axial thrust forces generated by the pressure device, which consists of the preloaded rubber spring and the slide, are also prescribed.

Step 2. The relationship between the OSR and the crank angle is kinematically evaluated according to Equation (3).

Step 3. According to the OSR, the normal force is calculated by:

$$N_1 = \frac{F_{tr}^{(1)}}{\cos\theta_1} \tag{9}$$

where N_1 is the normal force to the contact area between the drive rotor and the counter rotor, and $F_{tr}^{(1)}$ is the thrust force by the frontal pressure device.

Step 4. The radius of the contact circle, the maximum contact pressure and shear stress vector, and the creep rate at the infinitesimal location within the contact area are calculated based on the Hertzian contact theory.

Step 5. The unknown variable (the speed of the counter rotor assembly) is determined from the equilibrium equation for the axial torque, based on the free-body

diagram of the drive rotor on which the input torque acts. The energy efficiency between the drive rotor and the associated counter rotor is calculated by:

$$\int_{A_1} (\mathbf{r}_1 + \rho_1) \times \tau_1 dA_1 - T_1 = 0 \tag{10}$$

where T_1 is the input torque.

Step 6. The follower angle of the four-bar linkage from Equations (1) and (2), and the normal force generated by the rear pressure device is calculated as follows:

$$N_2 = \frac{F_{tr}^{(2)}}{\cos\theta_2} \tag{11}$$

where N_2 is the normal force to the contact area between the drive rotor and the counter rotor and $F_{tr}^{(2)}$ is the thrust force by the frontal pressure device.

Step 7. Through the processes in Steps 4 and 5, the speed of the driven rotor is solved from the equilibrium equation for the axial torque based on the free-body diagram of the driven rotor. The counter rotor and the associated driven rotor are calculated by:

$$\int_{A_1} (\mathbf{r}_1 + \rho_1 - \mathbf{a}_1) \times \tau_1 dA_1 + \int_{A_2} (\mathbf{r}_2 + \rho_2 - \mathbf{a}_2) \times \tau_2 dA_2 = 0 \tag{12}$$

$$\int_{A_2} (\mathbf{r}_2 + \rho_2) \times \tau_2 dA_2 - T_2 = 0 \tag{13}$$

$$\eta = \frac{\omega_2 T_2}{\omega_1 T_1} \tag{14}$$

where T_2 is the output torque and η is the energy efficiency.

Step 8. The transmission performance (p-v values, the life time based on the Lunderberg method (Frederic W. Heilch III, 1983), the reactive forces at the pivots and joints of the four-bar linkage, etc.) is simultaneously evaluated with the overall energy efficiency.

3. DESIGN FOR BICYCLE CVT

Figure 4 shows the layout of the BCVT. Power is supplied by a rider or electrical motor. The BCVT has a front-belt system connecting the pedals and the input pulley of the CVU. The CVU is installed on the bicycle frame. It also has a rear-belt system connecting the output pulley of the CVU and the rear wheel. The speed controller is kinematically designed to change the crank angle by controlling the handlebars. Crank torque must be small enough so that the speed controller can be operated easily by hand.

A flowchart of the design procedure is shown in Figure 5. For any given design specification, the design procedure is divided according to kinematic design and kinetic design. The design specifications include input power, input speed, and the range of the OSR. For bicycle

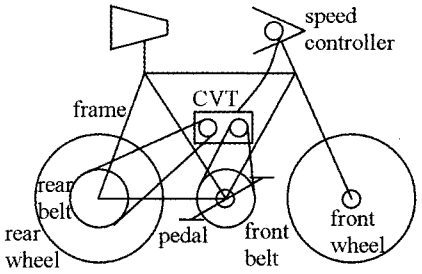

Figure 4. Layout of BCVT.

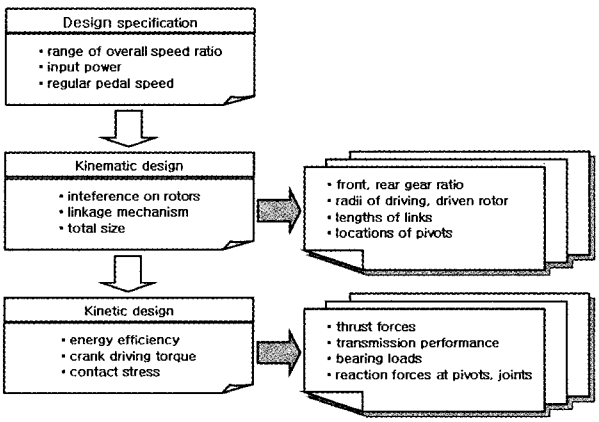

Figure 5. Schematic diagram of design procedure.

use, the range of the OSR, the input power and the regular input speed are given as 1.0–4.5, 100 Watts, and 6 rad/s, respectively.

In the kinematic design, to satisfy the given OSR and to avoid interference among components of the CVU, the belt ratio design variables, the relative sizes of the traction drives, and the relative dimensions of the links, are obtained using the direct search method (Table 1). According to the design specifications, the overall size of the installed CVT can fit within a 244 × 125 × 160 mm^3 space above the pedals.

The kinetic design for the given power and speed is simulated for the following reasons: to avoid occurrence of excessive crank torque and contact stress; to satisfy the size constraints; and to maximize the average energy efficiency in the operating speed range, the dimensions of the CVU, and the thrust forces of the pressure devices. The range of input torque and speed for a primary bicycle operating line is assumed to be 6–20 Nm and 3–9 rad/s, respectively. The mean values are 13 Nm and 6 rad/s.

4. TRANSMISSION PERFORMANCES

A contour diagram of the average efficiency for the prescribed thrust forces of 500 N and 300 N at the frontal and rear rotor pair, respectively, is shown in Figure 6. The

Table 1. Design variables.

Contents	
■ belt system	
- front speed ratio	: 5.0
- rear speed ratio	: 0.2
■ radii of traction rotor (mm)	
- driving	: 53.3
- driven	: 71.5
■ lengths of 4-bar linkage (mm)	
- crank	: 38.2
- follower	: 19.3
- coupler	: 99.2
- fixed link	: 129.8
- angle of fixed link (deg)	: 0
■ thrust forces of pressure device (kN)	
- drive	: 0.45
- driven	: 0.25

efficiency is averaged according to the range of the speed ratio at each input torque and input speed. The average efficiency is about 0.93. Figure 7 shows that the variation with respect to the range of the speed ratio at the rated values changes little. This indicates that the proposed CVT is very suitable for a transmission system with a wide speed ratio. Figure 8 shows the magnitude of the torque necessary to operate the crank arm while the speed is varied continuously and the rider is pedaling according to the rated values. The magnitude is about 5.0 Nm which is too large for the rider to handle by hand grip torque. But if the rider ceases pedaling at the instant of the speed variation, there is no torque to operate the crank arm. Besides, the reactive force and moment applied at the

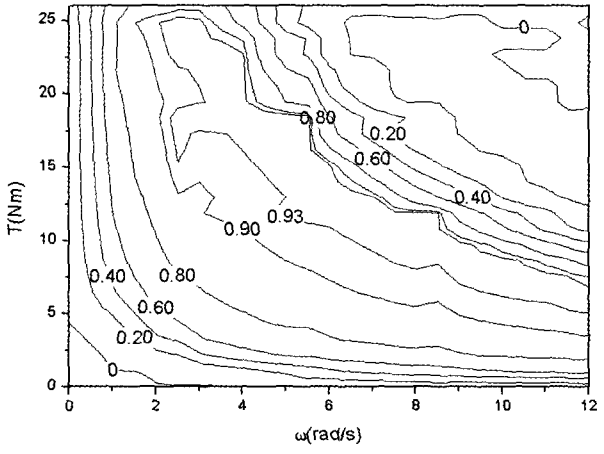

Figure 6. Average energy efficiency under dry friction with respect to torque and speed ($\mu = 0.2$, $F_{tr}^{(1)}$ =500N, $F_{tr}^{(2)}$ =300N).

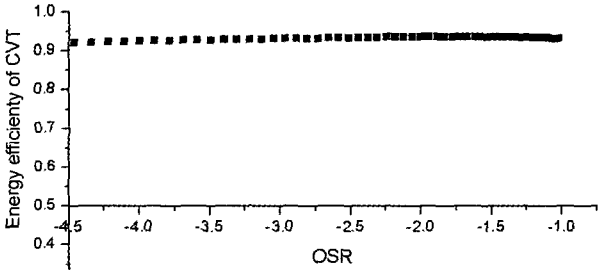

Figure 7. CVT energy efficiency (T_i = 13 Nm, Ω_i = 6 rad/s).

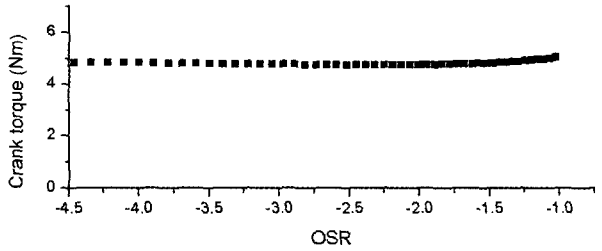

Figure 8. Crank torque.

linkage pivots are 725 N and 1.6 Nm respectively, which are compatible with the small size of the four-bar linkage. The maximum shear stresses under the worst case loading conditions of the rated values are 485.6 MPa at the drive rotor and 96.3 MPa at the driven rotor. The lifetimes based on the Lunderberg-Palmgreen method are calculated to be of nearly infinite value, 8.61×10^{14} hours and 1.0×10^{20} hours at the drive and driven rotor, respectively. The reliability of the ISCVT can be expected to be excellent.

5. ROAD SIMULATION

To check the gradeability of the ISCVT, a road simulation module having a running road with 7 regimes was assumed as shown in Figure 9. Figures 9(b)–(d) show the prescribed values of the rear wheel speed, the pedal torque, and the OSR in riding mode in Figure 9(a).

Starting at rest, the test rider increases the pedal torque linearly, up to 10 Nm, in Regimes A and B. He maintains speed in the lowest mode (OSR=1) in Regime A and changes it to the highest mode (OSR=4.2) in Regime B. The cycle speed is accelerated up to 0.1 g in Regimes A and B. He decreases the pedal torque in Regime C, maintaining a constant speed. In Regimes D and E, the road is inclined at an angle of 2.9°. As soon as the rider enters the inclined road, he changes speed to the minimum in Regime D and maintaines a constant speed, 0.69 m/s in Regime E. Entering the flat road, he changes speed to a maximum in Regime F and maintains constant speed in Regime G.

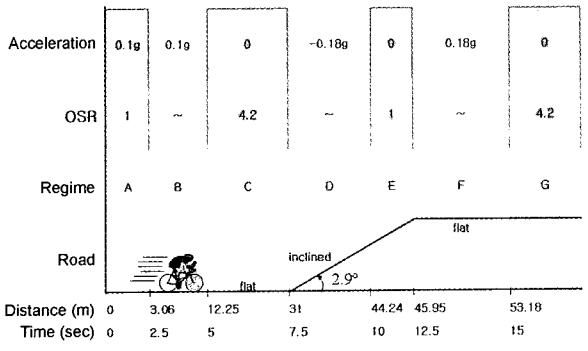

(a) Riding mode

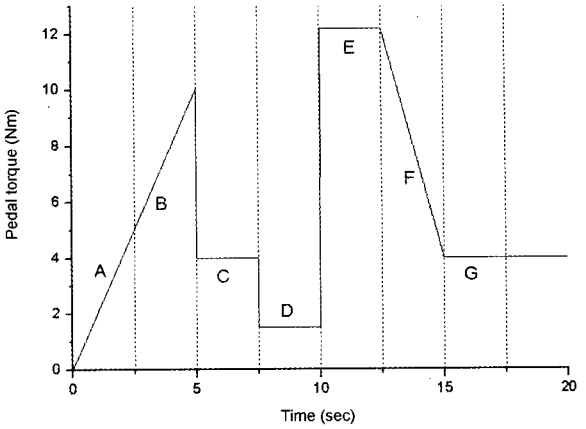

(c) Precribed pedal torque

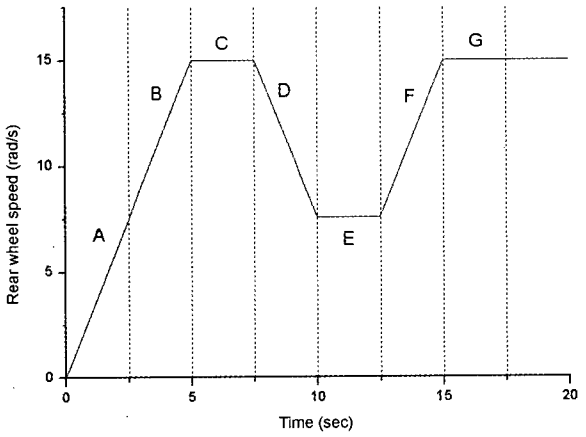

(b) Prescribed rear wheel speed

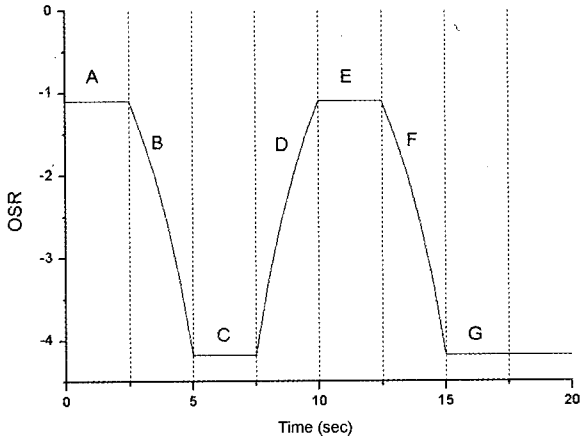

(d) Prescribed OSR

Figure 9. Simulated driving pattern.

His pedal speed can be decreased since the magnitude of OSR is increased. For example, at 2.5 sec, the bicycle speed is 7.5 rad/s × 0.5 m = 3.75 m/s and the pedal speed is 6.82 rad/s because OSR is 1.1. The pedal torque that he is applying is 5 Nm. Therefore, he applies the power of 5 Nm × 6.82 rad/s = 34.1 Watts, which corresponds in Figure 11 with the time of 2.5 sec. But at the time of 5.0 sec, the bicycle speed is 15 rad/s × 0.5 m = 7.5 m/s and the pedal speed is calculated to be 3.57 rad/s. The pedal torque that he is applying is 10 Nm. Therefore, he applies a power of 10 Nm × 3.57 rad/s = 35.7 Watts, which corresponds in Figure 12 with the time of 5.0 sec. When he enters in the inclined road, he has some inertia. He need not pedal but uses his own kinetic energy for some distance. When the reserved energy is consumed, the wheel speed is decreased and he must apply some power by pedaling to maintain the speed and traverse the inclined road. So, in Figure 9(c), the jump of pedal torque indicates the resumption of pedaling.

The relationship of the given riding mode to the power

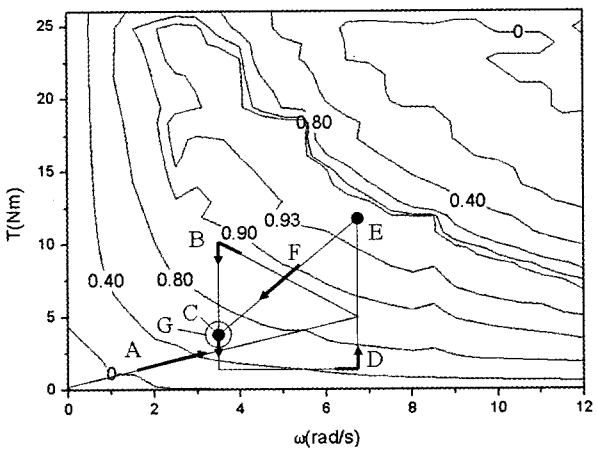

Figure 10. Riding mode with respect to torque and speed.

efficiency with respect to the pedal speed and the pedal torque is shown in Figure 10. The CVT efficiencies of the flat-road riding mode are in the region of 0.1–0.9 and

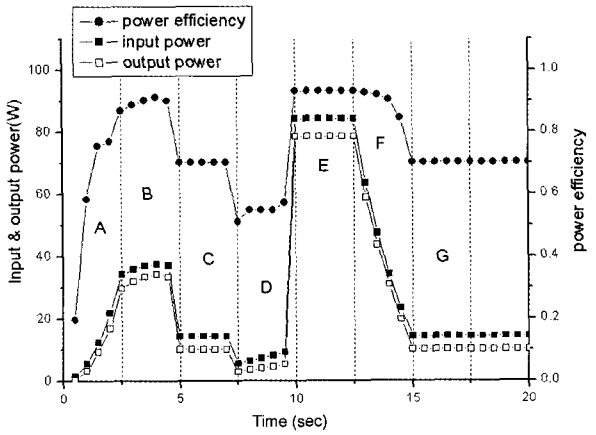

Figure 11. Power efficiency, input power, and output power (constant driving thrust force = 0.5 kN, constant driven thrust force = 0.3 kN).

those of the inclined-road riding mode are higher, above 0.93. Thus, the CVT efficiencies are appropriate for riding on an inclined road, whereas less appropriate for riding on a flat road. The power efficiencies, input power and output power are shown in Figure 11. This figure shows that the efficiencies in Regimes A, C, D, and G (start-up and constant-speed modes) are poor in relation to those in Regimes B and E (acceleration and incline modes). In Regime E, the maximum power, above 80 Watts, is applied. The reason that poor efficiencies are obtained in those regimes results from the fact that thrust forces are constant but the pedal torque varies. Thus, it is thought that a device generating constant thrust forces is inappropriate for both flat- and inclined-road riding modes. Accordingly, a mechanism by which the pressure is proportionally generated to the shaft torque is recommended.

6. CONCLUSIONS

In this paper, we presented the design results and analytical investigations of a newly developed ISCVT for a bicycle. Through a kinetic analysis, we examined the overall energy efficiency, transmission performances, and gradeability of the bicycle with the ISCVT. The overall size of the ISCVT satisfying the design specifications is $244 \times 125 \times 160$ mm^3, which is small enough to be installed in the middle part of a bicycle above the pedals. The distribution of efficiency calculations as a function of the input torque and input speed showed that when the input power is in the 40–100 Watt range, the efficiency is high, 0.9–0.95, but below 40 Watts, the efficiency is less than 0.8. The variation according to the range of OSR is very small. Low efficiencies are obtained in the riding mode using low power. To improve the efficiencies, a device having proportional torque is recommended.

REFERENCES

Carter, J. and Miller, D. (2003). The design and analysis of an alternative traction drive CVT. *Transmission & Driveline Systems Symposium 2003*, SAE Technical Paper 2003-01-0970, March, Detroit, Michigan, USA.

Frederic, W. Heilch III, Eugene, E. Shube (1983). *Traction drives; Mechanical Engineering Series*. Marcel Dekker Inc. 177–205.

Kim, J., Park, F. C., Park, Y. and Shizou, M. (2002). Analysis and control of a spherical continuously variable transmission. *Mechanical Design* **124**, **1**, 21–29.

Kim, J. and Choi, K. H. (2003). Spin loss analyisis of friction drives: spherical and semi-spherical CVT. *Int. J. Automotive Technology* **4**, **4**, 165–172.

Lee, H. and Kim H. (2003). CVT ratio control for improvement of fuel economy by considering power-train response lag. *KSME International Journal* **17**, **11**, 1725–1731.

Norton, R. L. (2000). *Machine Design–An Integrated Approach*, 2nd edn., Prentice-Hall Inc., N. J.

Pfiffner, R., Guzzella, L. and Onder C. H. (2003). Fuel-optimal control of CVT powertrains. *Control Engineering Practice* **29**, **11**, 329–336.

Ryu, J. H., Seong, S. H. and Park, N. G. (2002). A continuously variable transmission having a four-bar linkage and spherical rotors. *Spring Conference Proc. Korean Society Automotive Engineers*, 889–896, May 30-June 1, Jeju, Korea.

Ryu, J. H., Seong, S. H. and Park, N. G. (2002). An introduction of an infinitely variable transmission using concave and convex sphered traction drive for electric vehicle use. *19th Worldwide Battery, Hybrid and Fuel Cell Electric Vehicle Symposium & Exhibition* 1443–1450, October, Busan, Korea.

Ryu, J. H., Kim, Y. K. and Park, N. G. (2002). A split power continuously variable transmissions (SPCVT) for bicycle use. *Proc. Small Engine and Transmission Conference 2002*, 20024265(JSAE), October, Kyoto, Japan.

Shoji, A. and Kawashima G. (2002). The Development of the traction drive mechanism made of the plastic magnet, *Proc. Design Engineering Technical Conferences and Computers and Information in Engineering Conference 2003*, September, Illinois, USA.

Tanaka, H. and Eguchi, M. (1991). Speed ratio control of a half-toroidal traction drive CVT. *JSME* 91-0375 B, 203–211.

Tanaka, H. and Machida, H. (1996). Half-toroidal traction-drive continuously variable power transmission. *Engineering Tribology* **210**, **3**, 205–212.